Adsorption 11: 259–273, 2005

Diffusion in Surface Modified ZSM-5 Studied Using the ZLC Method

W.L. DUNCAN AND K.P. MÖLLER*
Catalysis Research Unit, Department of Chemical Engineering, University of Cape Town, Private Bag, Rondebosch, 7701, Republic of South Africa
km@chemeng.uct.ac.za

Abstract. Deposition of silane on a zeolite's external surface is a well established method of increasing its shape selective properties by modifying diffusion resistances. In this work the intracrystalline diffusivity of cyclohexane in both a parent and silanized ZSM-5 samples were measured using the zero length column technique. It was found that the apparent intracrystalline diffusivity did indeed decrease in the modified samples. Models based on a surface barrier approach to describe pore mouth narrowing and an increase in intracrystalline tortuosity as a result of pore blockage were used to interpret the experimental data. It is found that the data correspond most consistently with the model describing pore blockage.

Keywords: characterization of zeolite properties, mathematical diffusion models, experimental diffusion data, intraparticle diffusion, silanization

1. Introduction

The deposition of alkoxysilanes to increase the shape selectivity of zeolite catalysts has been extensively studied (Hibino et al., 1989, 1993; Kim et al., 1996; Čejka et al., 1996; Röger et al., 1998; Weber et al., 2000; Manstein et al., 2002). While many authors believe that the predominant reason for this change in shape selectivity is a transport rate reduction due to narrowing of the pore entrances (Kim et al., 1996), some believe that blockage of the pore mouths is a factor (Weber et al., 2000; Röger et al., 2001). Diffusion studies have been carried out on these silanized catalysts, but not in sufficient quantitative detail to draw any other conclusion than that the transport rate had indeed decreased after silanization (Čejka et al., 1996). Theoretical studies using stochastic models on finite grids have also been performed to determine the behavior of a sorbate with surface modifications (Theodorou and Wei, 1983), but the two dimensional nature of the theoretical systems causes quantitative extrapolation to experimental systems to be questionable. Nevertheless this work shows that the effective diffusivity depends on the degree of pore blockage.

*To whom correspondence should be addressed.

This paper presents the results of a detailed study, using the zero length column method (Eic and Ruthven, 1988), into the diffusion characteristics of cyclohexane in ZSM-5 modified by the liquid phase deposition of tetraethoxy silane (TEOS). These results may be compared to those presented in Duncan and Möller (2000) for unmodified ZSM-5. The parent sample of this paper is Sample C of that work. Mathematical models speculating the system behavior are developed, indicating possible trends that are looked for in the experimental data.

Cyclohexane should be an appropriate choice to detect pore mouth narrowing effects, since its size is similar to that of the ZSM-5 pores, yet it is flexible and should thus be able to enter the pore mouths if they are narrowed. The distortion required to pass through a constricted pore mouth should reveal itself as a surface barrier type phenomenon.

2. Theoretical

2.1. The Standard ZLC Analysis

The most commonly applied mathematical model for the analysis of ZLC desorption curves is that presented

by Eic and Ruthven (1988). The system is assumed to conform to the assumptions of spherical, monosized sorbent particles, Fickian diffusion, a linear (Henry) adsorption isotherm and a well-mixed fluid phase with negligible interstitial hold-up. This results in the equation

$$\frac{C}{C_0} = 2L \sum_{n=1}^{\infty} \frac{\exp\left(-\beta_n^2 \tau\right)}{\beta_n^2 + L(L-1)} \tag{1}$$

where

$$\tau = \frac{D}{R^2} t \tag{2}$$

$$L = \frac{F R^2}{3 V_s K D} \tag{3}$$

and β_n are given by the roots of

$$\beta_n \cot \beta_n + L - 1 = 0 \tag{4}$$

For the case of large L (i.e. large dominance of diffusion over convective transport from the particle surface) and at long times, the solution simplifies to the form

$$\ln \frac{C}{C_0} = \ln \frac{2}{L} - \pi^2 \tau \tag{5}$$

2.2. *Surface Barrier Analysis for the ZLC*

Pore mouth narrowing effects are represented by using a surface barrier model (Kärger and Ruthven, 1992), i.e. a first order desorption rate process at the surface of the catalyst particle:

$$\text{rate} = k_s(\text{area})(q|_R - KC) \tag{6}$$

The barrier rate constant k_s is the ratio of the effective diffusivity of the solid surface 'film' and its thickness (Kärger and Ruthven, 1992).

The boundary condition for Fick's Law at the particle surface is then

$$FC = \frac{3 k_s V_s}{R}(q|_R - KC) \tag{7}$$

or, in dimensionless form,

$$\left(\frac{D}{k_s R} + \frac{1}{L}\right) \left.\frac{\partial U}{\partial X}\right|_1 + U|_1 = 0 \tag{8}$$

This may be compared to the corresponding condition for the standard ZLC model, i.e.

$$\frac{1}{L} \left.\frac{\partial U}{\partial X}\right|_1 + U|_1 = 0 \tag{9}$$

from which it is clear that the characteristic parameter in the surface barrier model (Eq. (8)) is L_s, where

$$\frac{1}{L_s} = \frac{1}{L} + \frac{D}{k_s R} \tag{10}$$

which is analogous to L in the standard model. The solution for the desorption curve is

$$\frac{C}{C_0} = 2\frac{L_s^2}{L} \sum_{n=1}^{\infty} \frac{\exp\left(-\beta_{sn}^2 \tau\right)}{\beta_{sn}^2 + L_s(L_s - 1)} \tag{11}$$

where β_{sn} are calculated as in Eq. (4) with L replaced by L_s:

$$\beta_{sn} \cot \beta_{sn} + L_s - 1 = 0 \tag{12}$$

For complete surface barrier control Eq. (6) may be combined with the particle sorbate balance, realizing that q is a function of t only,

$$\frac{d(q V_s)}{dt} = -FC \tag{13}$$

to show that the desorption curve is given by a exponential decay with an initial value less than unity:

$$\frac{C}{C_0} = \alpha \exp\left(-\alpha \frac{F}{K V_s} t\right) \tag{14}$$

where

$$\frac{1}{\alpha} = 1 + \left(\frac{F}{K V_s}\right)\left(\frac{R}{3k_s}\right) \tag{15}$$

For the limiting case $k_s \to \infty$ (i.e. equilibrium control with no surface barrier), $\alpha \to 1$ and Eq. (14) becomes

$$\frac{C}{C_0} = \exp\left(-\frac{F}{K V_s} t\right) \tag{16}$$

which is, correctly, the equation describing equilibrium controlled desorption as given in Eic and Ruthven (1988).

Sample desorption curves calculated from Eq. (11) are shown in Fig. 1. It is clear that the surface barrier

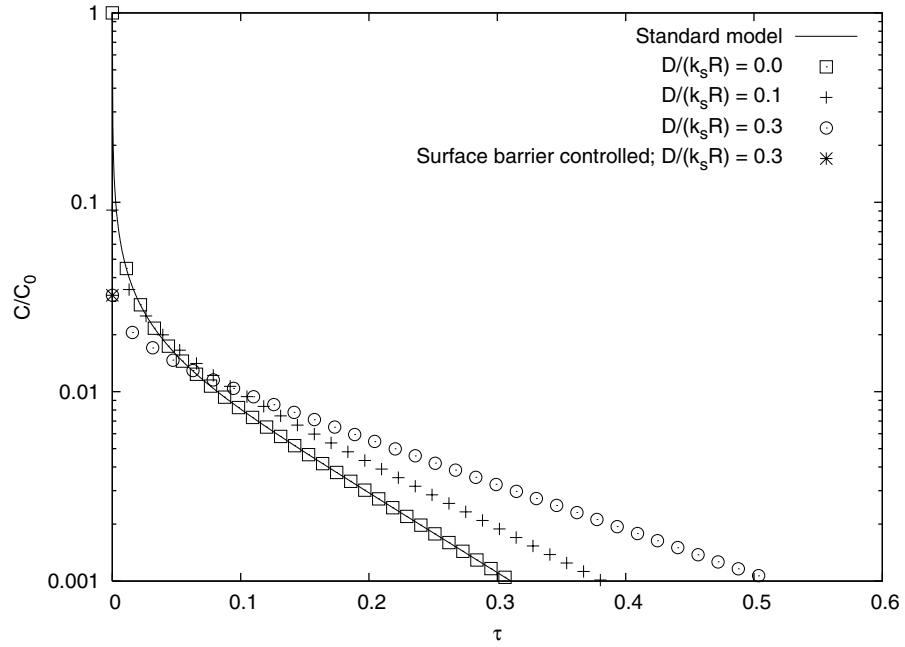

Figure 1. Desorption curves for the diffusion with surface barrier model (Eq. (11)) for various $D/(k_s R)$ as shown and $L = 100$. The standard model and initial point of the surface barrier controlled curve are shown for verification.

has a significant effect on the linear tail of the curve, from which the diffusivity is normally obtained by the long time method. The slope of the tail decreases with increasing surface barrier resistance. This is a result of the eigenvalues being calculated using L_s: although L is large ($L = 100$), the significant value of $D/(k_s R)$ causes that L_s is not large enough that $\beta_{s1} \simeq \pi$, although it would appear that way from the intercept of the linear region of the desorption curve if the standard approach were being used. For example, for the case $D/(k_s R) = 0.1$ and $L = 100$, it is found that $L_s = 5$ and so $\beta_{s1} \simeq 2.57$. If the curve were analyzed using the standard long time method with the assumption $\beta_1 = \pi$, the diffusional time constant would be calculated at 67% of its 'true' value, while the apparent value of L would be 106.

Figure 2 shows that the only visible difference between the desorption curves of the two models is that the surface barrier case undergoes a more rapid initial concentration decrease. It is unlikely that this effect would be experimentally noticeable, particularly considering that the effect is exaggerated as outlined above. The true short time behavior is likely to be an exponential decay, similar to the liquid phase model (Brandani and Ruthven, 1995).

2.2.1. Behaviour of the Intercept with Flow Rate. The long time approximation to Eq. (11), for the case of non-large L_s, is

$$\ln \frac{C}{C_0} = \ln \left[\frac{2L_s}{\beta_{s1}^2 + L_s(L_s - 1)} \cdot \frac{L_s}{L} \right] - \beta_{s1}^2 \tau \quad (17)$$

For large values of L (at high flow rates, for example), $L_s \simeq k_s R/D$, which is constant with respect to flow rate, implying that β_{s1} is constant with F. Thus, at high flow rates

$$\ln \frac{C}{C_0} = \ln \frac{\eta}{L} - \beta_{s1}^2 \tau \quad (18)$$

where

$$\eta = \frac{2L_s^2}{\beta_{s1}^2 + L_s(L_s - 1)} \quad (19)$$

which does not change with purge rate. This is the same form as the standard large L, long time approximation (Eq. (5)).

Thus, when a system with a significant surface barrier resistance is analyzed using the standard model and the long time solution method, an apparent L is obtained that is linear with flow rate (passing through

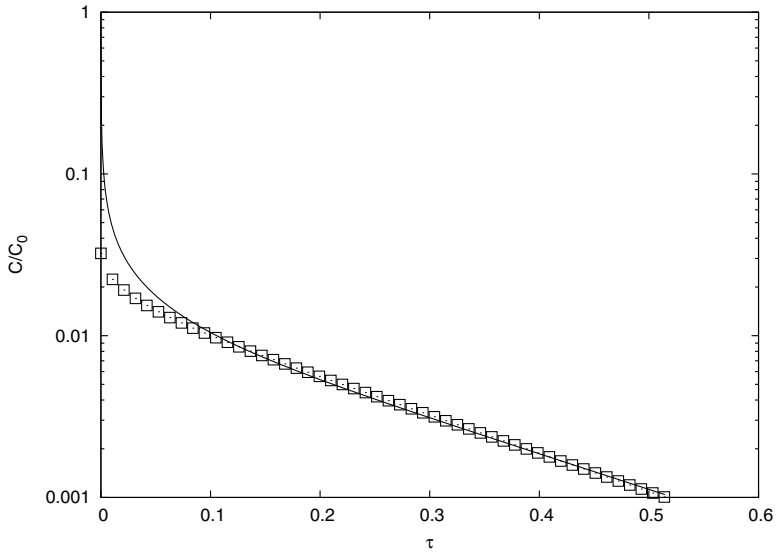

Figure 2. Fit of the standard model (lines) to the surface barrier model (points) for $D/(k_s R) = 0.3$ and $L = 100$.

the origin) at large flow rates, but has more complex behavior at low flow rates. This behavior would likely be very difficult to detect experimentally.

2.2.2. The Effect of a Surface Barrier on Activation Energy. Intuitively, it may be expected for the presence of an additional, series resistance to diffusive transport to increase the apparent diffusional activation energy. The above analysis shows, however, that such a conclusion is far from obvious. To investigate any such effect, the temperature dependence of β_{s1}, which is the parameter the surface barrier truly affects, must be considered.

The limiting value of $\beta_1 = \pi$ occurs at high values of L (high flow rates). The analogous limiting value of β_{s1} similarly occurs at large values of L, such that $L_s \simeq k_s R/D$ and β_{s1} is independent of purge rate. The eigenvalues of the model are then given by the roots of

$$\beta_{sn} \cot \beta_{sn} + \frac{k_s R}{D} - 1 = 0 \tag{20}$$

It is reasonable to assume that transport across the surface barrier is an activated process, so k_s follows an Arrhenius temperature dependency:

$$k_s = k_{s\infty} e^{-\frac{E_{as}}{R_g T}} \tag{21}$$

where E_{as} is the activation energy for penetrating the barrier. Additionally expressing the diffusion coefficient as an explicit function of temperature, one may write Eq. (20) as

$$\beta_{sn} \cot \beta_{sn} + \frac{k_{s\infty} R}{D_\infty} e^{\frac{E_a - E_{as}}{R_g T}} - 1 = 0 \tag{22}$$

which implicitly gives the temperature dependence of the eigenvalues. Inspection of this expression reveals that

- $E_a > E_{as} \Rightarrow \frac{k_s R}{D}$ decreases as T increases;
- $E_a < E_{as} \Rightarrow \frac{k_s R}{D}$ increases as T increases;
- β_{s1} increases as $\frac{k_s R}{D}$ increases.

Thus the initial eigenvalue increases with temperature for the likely situation $E_a < E_{as}$, implying that the apparent diffusivity increases more strongly with temperature than the true diffusivity, so it is possible that a larger apparent activation energy would be observed for a system with a surface barrier.

Figure 3 shows the variation of β_{s1} over the temperature range typical for the cyclohexane/ZSM-5 system used in this work. The activation energy of the surface barrier was chosen to be approximately twice that of the activation energy of diffusion, while the ratio of diffusion to surface barrier transport time $k_{s\infty} R/D_\infty$ was chosen largely to give apparently reasonable values of the second term in Eq. (22); it represents the case in which transport across the surface barrier is orders of magnitude slower than that within the sorbent particle.

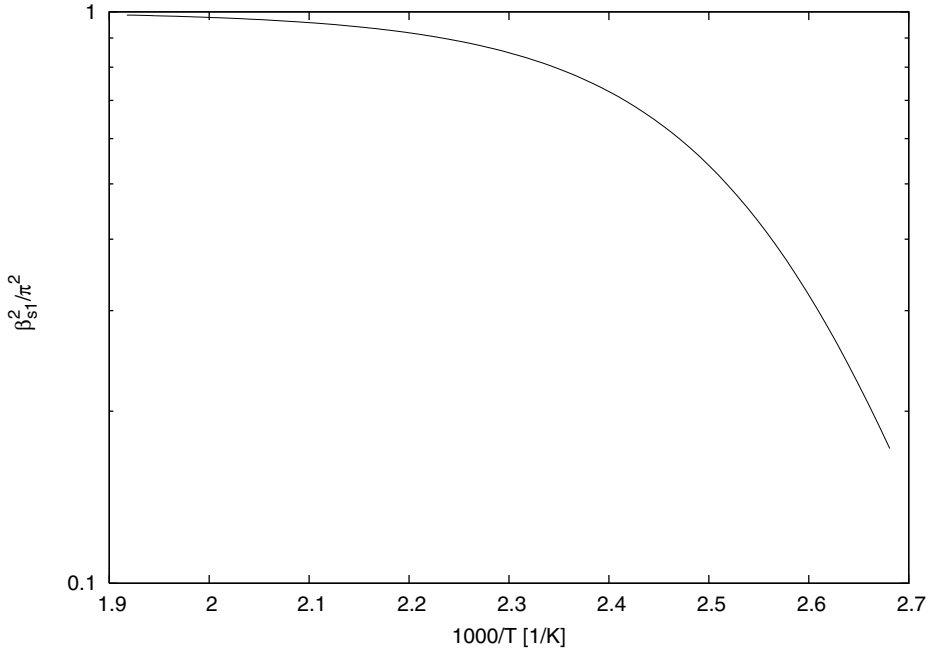

Figure 3. Variation of the initial eigenvalue of the surface barrier model with temperature for $E_a - E_{as} = -55\,\text{kJ/mol}$ and $k_s R/D = 10^8$.

The figure indicates that the effect of the surface barrier on the Arrhenius plot for the diffusion coefficient, if significant, is unlikely to simply increase the slope of the usual straight line. Thus the temperature dependence of the diffusivity should appear to deviate from the Arrhenius form if the surface barrier has a major effect.

It is thus probably safe to conclude that the presence of a surface barrier to diffusion would not significantly increase the measured diffusional activation energy, since the Arrhenius plot of the diffusion coefficient is likely to deviate from linearity for a significant surface barrier resistance.

2.2.3. The Effect of a Surface Barrier on Adsorption Constant. When using the standard model and long time solution method to analyze a desorption curve for a system with a surface barrier, Eq.'s (5) and (18) can be compared to determine the deviation that could be expected in the apparent parameters so obtained. Considering the slope and intercept terms, it may be seen that the apparent value of D is given by the expression

$$D_{app} = \frac{\beta_{s1}^2}{\pi^2} D \tag{23}$$

and L_{app} by

$$L_{app} = \frac{L}{L_s^2}\left[\beta_{s1}^2 + L_s(L_s - 1)\right] \tag{24}$$

from which it may be derived that, for large flow rates,

$$\frac{K_{app}}{K} = \frac{\beta_{s1}^2}{\pi^2 L_s^2}\left[\beta_{s1}^2 + L_s(L_s - 1)\right] \tag{25}$$

The relationship is plotted in Fig. 4.

It may be seen that, for a wide range of values of L_s (and hence surface barrier resistance), the value of K determined by application of Eq. (5) is not significantly different to the true value.

2.3. Analysis of Pore Blockage

Two simplistic, extreme cases will be considered, the real description probably lying between the two.

2.3.1. Decrease in Surface Area for Flux. For the first case, assume that pore blockage results in the surface area available for flux of the sorbate out of the sorbent particle being reduced (see A of Fig. 5). If the catalyst particle has a surface area A, define a factor

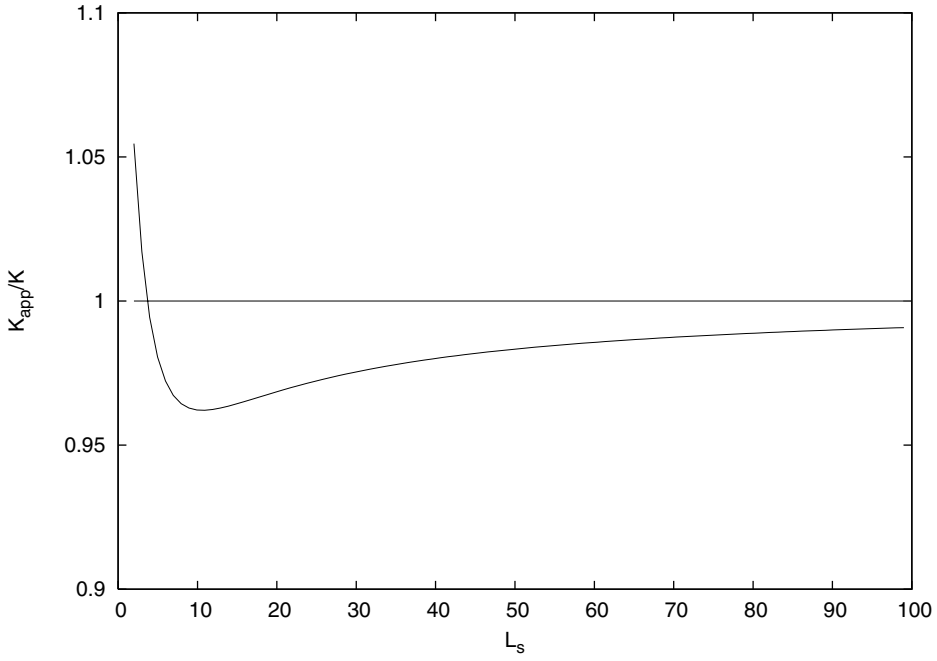

Figure 4. Error in apparent value of K relative to true value when using the standard analysis for a system influenced by a surface barrier.

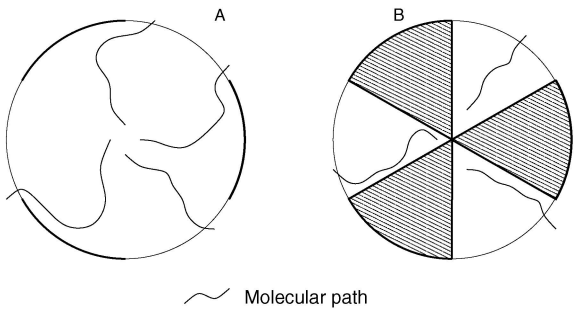

Figure 5. Representations of the pore blockage models showing which areas of the sorbent particle do not allow radial diffusive flux.

α ($0 < \alpha \leq 1$) such that the modified particle has an area $\alpha^2 A$ available for transport. The fluid phase mass balance is then modified from

$$D \left.\frac{\partial q}{\partial r}\right|_R + \frac{FR}{3V_s K} q|_R = 0 \tag{26}$$

to

$$D \left.\frac{\partial q}{\partial r}\right|_R + \frac{FR}{3\alpha^2 V_s K} q|_R = 0 \tag{27}$$

The model solution retains the same form as the standard model, except that L is replaced by L' where

$$L' = \frac{FR^2}{3\alpha^2 V_s K D} \tag{28}$$

The time scale of the experiment (i.e. the time constant D/R^2) is unchanged, while the convection term is altered. This agrees with the initial assumptions in that the bulk of the catalyst particle is unaffected and only the surface is modified. The boundary condition has been altered without changing the micropore mass balance.

It should be noted that a similar effect could be achieved by decreasing the volume of sorbent, increasing the purge flow rate or decreasing the adsorption constant K. Of these, only the change in K could be physically relevant to the silanization investigation, since it is possible that silanization could decrease the adsorption capacity of the sorbent. This seems unlikely, however, since the unmodified interior of the particle must be at the same concentration (KC) as if the surface were unmodified, from simple thermodynamic considerations. The surface may have a lower loading, but its capacity relative to the crystal interior is likely to be negligible.

This case will be referred to as model A.

2.3.2. Decrease in Total Area for Flux. For the second case, consider that the particle is made up of successive layers of differential shells, each of which has a similar fraction of its area blocked for flux in the same way as the surface was considered blocked in the case above. One may picture it as the blocked portions of the particle surface casting a 'shadow' toward the centre of the crystal (see B of Fig. 5). The general mass balance from which Fick's Second Law is derived has the form

$$\frac{\partial}{\partial t}\iiint_V q\,dV = -D\iint_A \nabla q\,dA \qquad (29)$$

for systems with a constant diffusivity. It is assumed that

$$\iint_{\alpha^2 A} \nabla q\,dA = \alpha^2 \iint_A \nabla q\,dA \qquad (30)$$

which is reasonable for an isotropic sphere, for which the diffusive flux should be constant at all points on the surface (i.e. q is a function of r only). It then follows that the diffusion equation for a 'partially non-porous' particle can be written as

$$\frac{\partial q}{\partial t} = \alpha^2 D\nabla^2 q \qquad (31)$$

The fluid phase mass balance takes the same form as the case described above (Eq. (27)).

The model for the ZLC desorption curve is then clearly

$$\frac{C}{C_0} = 2L'\sum_{n=1}^{\infty}\frac{\exp\left(-\beta_n'^2\alpha^2\tau\right)}{\beta_n'^2 + L'(L'-1)} \qquad (32)$$

where L' is defined as in Eq. (28) and β_n' are given by the roots of

$$\beta_n'\cot\beta_n' + L' - 1 = 0 \qquad (33)$$

Unlike the previous case, this model does show a change in the experimental time, by a factor α^2.

Note that the particle capacity does not decrease; q is still based on the total particle volume as usual. That is to say, all the pores are still accessible, but not all are amenable to flux. The flux whereby material diffuses out of the 'shaded' regions (in a non-radial direction) so as to exit the particle is not explicitly included in the model.

This case will be referred to as model B.

2.3.3. Effect of Pore Blockage on Measured Parameters. Inspection of dimensionless parameters L' and $\alpha^2\tau = \alpha^2 D/R^2$ shows that the difference between model B (Eq. (32)) and the standard model may be expressed as an increase in the representative dimension from the particle radius R to a tortuous length R/α. One may intuitively expect a diffusional trajectory like that shown in Fig. 6, with the presence of blocked pores causing molecules to diffuse longer distances within the crystal to exit into the gas phase, i.e. the diffusion path is made tortuous by blocking a fraction of the pore mouths. The diffusion time, and so the experimental time, should then increase. Thus the analysis gives the correct qualitative behavior.

Model A, however, in which only the surface of the crystal was assumed to be affected, indicates that there should not be an increase in the diffusional behavior of the system, only a modification of the convectional characteristics (as represented by L and L'). Although one would expect a decrease in the diffusional time constant, due to the extended diffusion path and thus time, this model should not be disregarded. It is in fact far more reasonable that only the pore entrances (i.e. the surface) are affected by silanization with a bulky agent like TEOS, rather than the entire pore, from the entrance to the centre of the crystal, as assumed in Eq. (32).

The most reasonable explanation of the effect of pore mouth blockage is that the true behavior lies between these two extremes. It is likely that the diffusional time

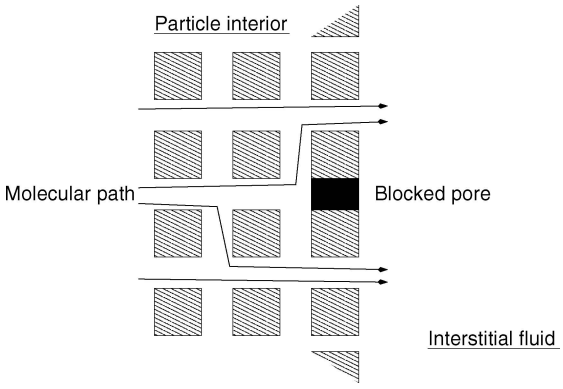

Figure 6. Conceptual diffusion paths inside a porous sorbent with a fraction of blocked pore openings.

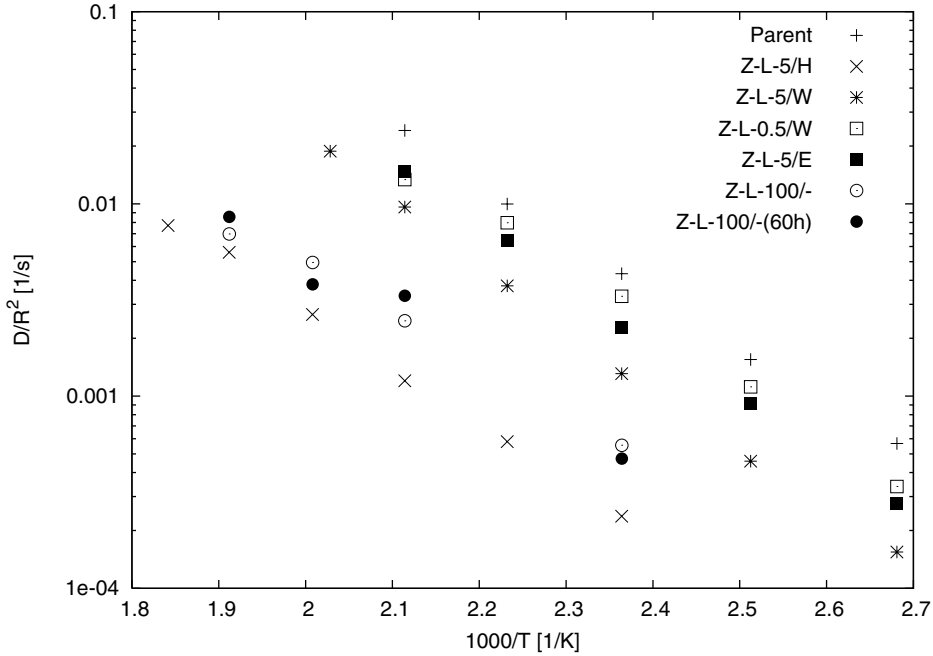

Figure 7. Arrhenius plot for the parent and all silanized ZSM-5 samples. Data have been averaged for each temperature.

constant is less severely affected than the dimensionless group L.

For a system conforming to model A and analyzed using the standard ZLC model, one should obtain the true diffusivity and underestimate the adsorption constant. For the case of model B, one should obtain a diffusivity D/α^2 and the true adsorption constant.

2.3.4. Limitations of the Pore Blockage Analyses. In addition to the inaccuracies in the model assumptions described above, there are a number of other implicit assumptions that should be highlighted:

multidimensional geometry as shown in Fig. 6, the problem is unlikely to remain one dimensional; there will be local concentration gradients in directions other than radial, which are not considered in the model solution;

no capacity decrease the derivation of Eq. (32) assumes that the sorbent volume available for adsorption does not decrease, contradicting the notion that parts of the crystal are inaccessible to the sorbate molecules.

The standard problem of modeling a system with a discrete channel system (like a zeolite) by using a continuum model is probably amplified in this situation.

3. Results and Discussion

The experimental method and modification procedure may be found in Duncan and Möller (2000).

Diffusional time constants for all modified samples are shown in Fig. 7. The decrease in diffusivity in the silanized samples is clear, particularly in the case of sample Z-L-5/H. Example desorption curves are shown in Fig. 8 for this and the parent catalyst at identical conditions, again clearly showing the difference in transport rate. The interpretation of the data for samples Z-L-100/- and Z-L-100/-(60h) is not clear (as explained below) and will be considered separately from the other samples, but they are shown for completeness.

The data for most of the sorbent samples appear consistent with the diffusion model and relatively easily interpreted, as can be seen in Figs. 8 and 9. The data for sample Z-5-L/H are particularly good, being represented by a single line on the Arrhenius plot for experiments run with 7 mg and with 2 mg. Note that Fig. 9 shows average data at each temperature for sample Z-L-0.5/W: the full data set shows the effect of a crystal size distribution, as discussed in Duncan and Möller (2002).

Comparison of Fig.'s 10 and 11 indicates the very good fit of the desorption model to the silanized catalyst data, while the data for the parent sample is somewhat curved. This indicates that sample Z-L-5/H has

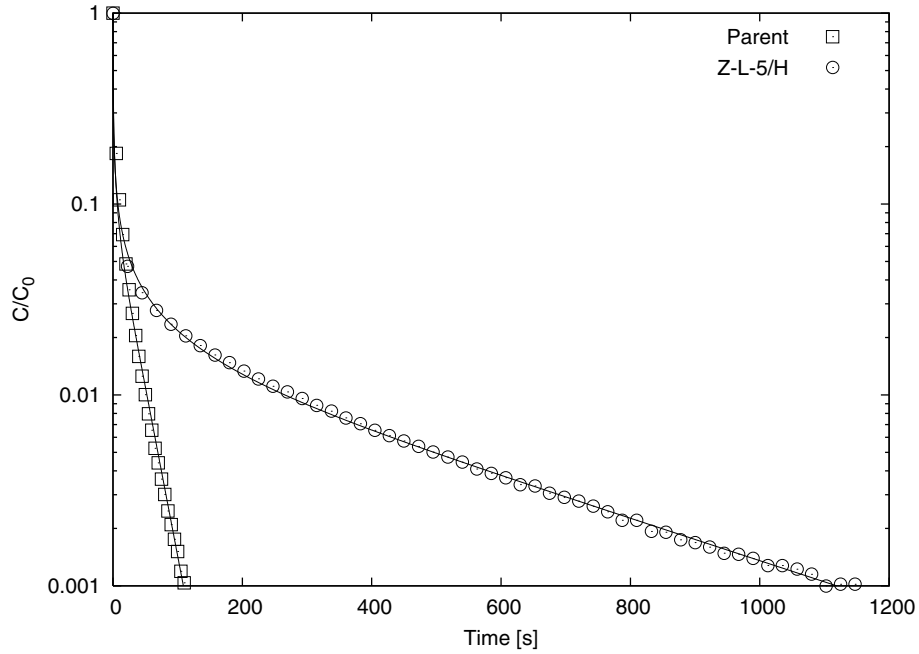

Figure 8. Experimental desorption curves and model fits for parent and silanized (Z-L-5/H) catalysts for identical conditions ($T = 150$°C, $F = 93.0$ ml/min, $C_0 = 191$ Pa).

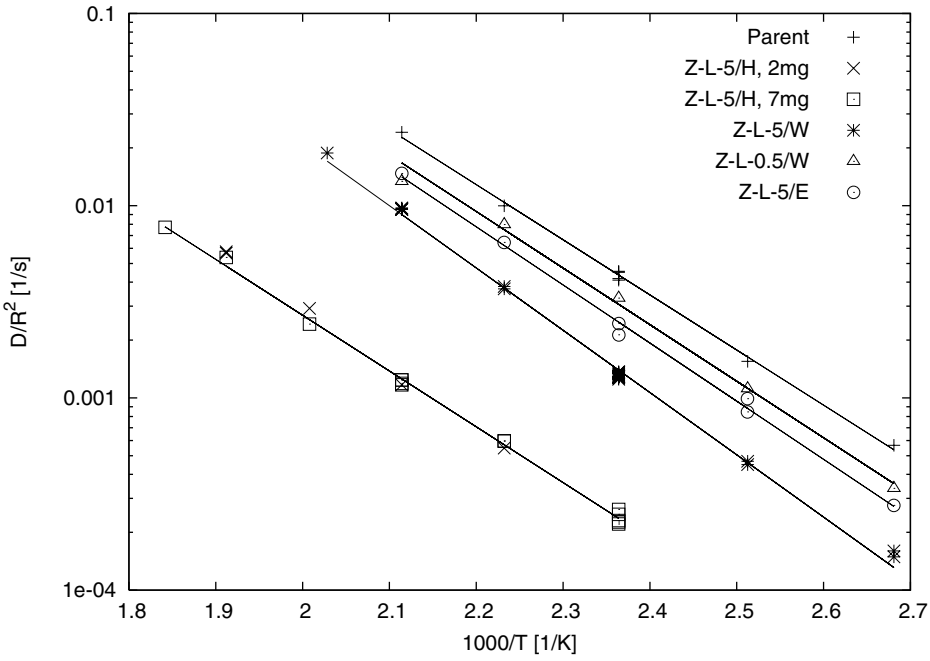

Figure 9. Arrhenius plot showing all data (except for sample Z-L-0.5/W, for which average data at each temperature are shown) for samples that have been modified with dilute TEOS.

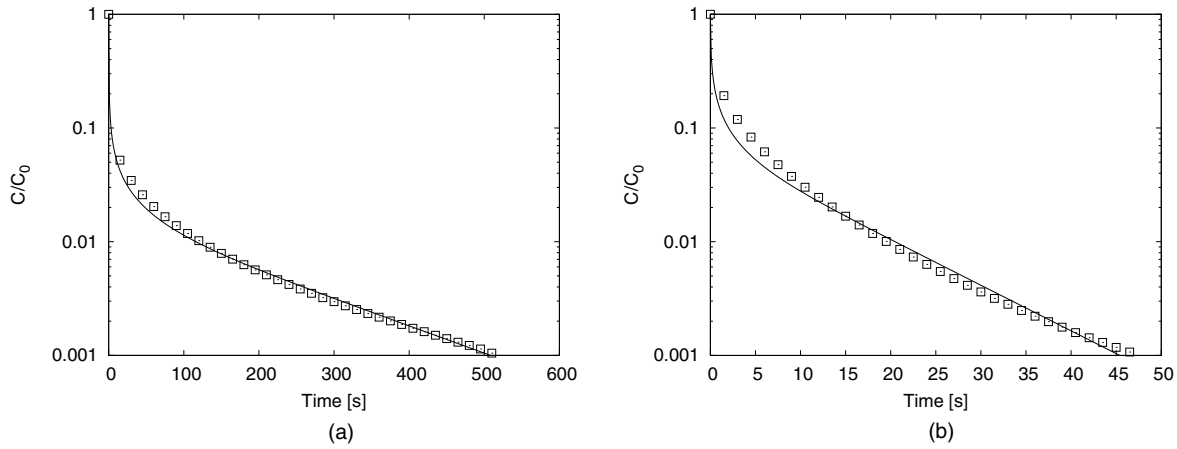

Figure 10. (a) $T = 100°C$, $F = 82.0$ ml/min, $C_0 = 191$ Pa and (b) $T = 175°C$, $F = 98.5$ ml/min, $C_0 = 191$ Pa. Sample desorption curves for the parent ZSM-5 sample at the conditions indicated.

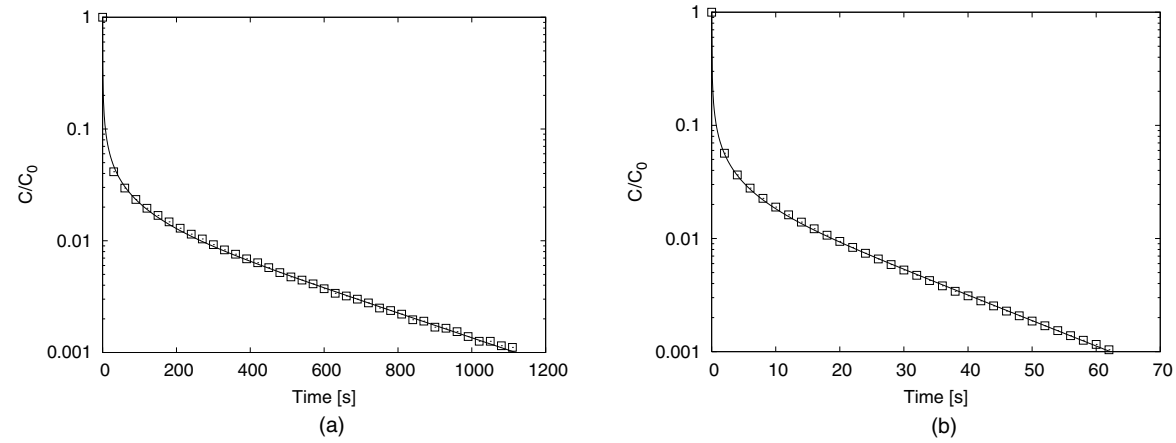

Figure 11. (a) $T = 150$℃, $F = 93.0$ ml/min, $C_0 = 191$ Pa and (b) $T = 250$℃, $F = 76.6$ ml/min, $C_0 = 287$ Pa. Sample desorption curves for 7 mg of sample Z-L-5/H at the conditions indicated.

a very narrow size distribution. It is possible that the presence of diluents during liquid phase silanization may disperse agglomerated particles (Weber, 1998), with the non-polar *n*-hexane providing the most suitable medium, thus providing the most uniformly sized sample.

3.1. Mechanism of Transport Rate Reduction

As illustrated in Fig. 8, silanization causes an increase in the time scale of a ZLC experiment. Thus model A, in which only the external surface area of the crystal was considered reduced for flux, may immediately be discounted. This is not surprising, since the principle behind increasing a catalyst's shape selectivity relies on an increase in diffusional resistance, which is characterized by the diffusional time constant. If L were to be interpreted as the initial (dimensionless) concentration gradient at the crystal surface (Ruthven and Brandani, 1997), it may be seen that its increase to L/α^2 is simply an increase of that gradient in order to obtain the same diffusive flux in spite of the reduced available area. This is because the mass balance must hold across the surface, i.e. the rate at which material leaves the surface must equal the rate at which it 'enters', since the surface itself has no volume and thus cannot accumulate any mass.

It has been shown above that the presence of a surface barrier could cause the temperature dependence of the

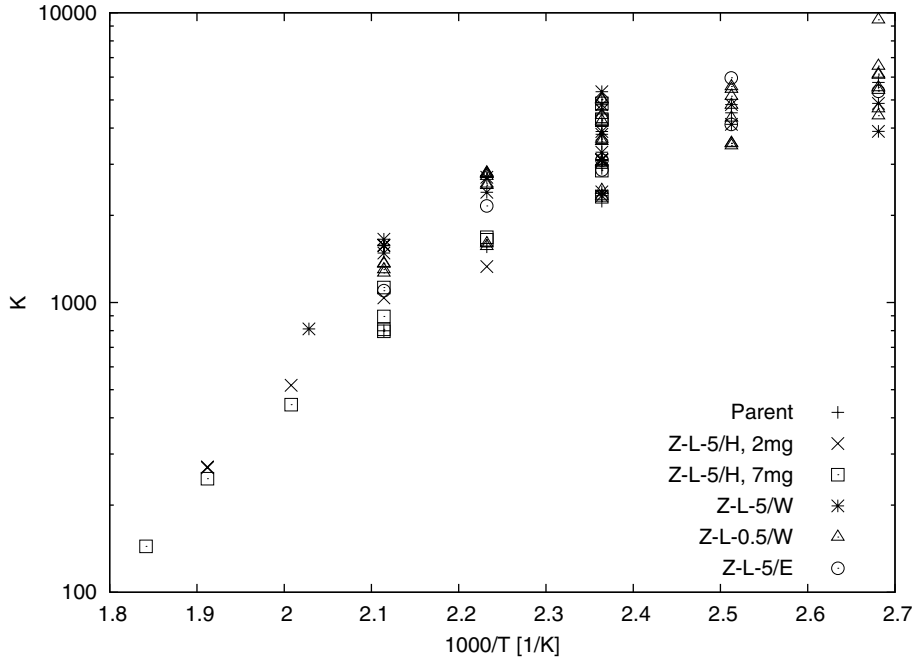

Figure 12. Van't Hoff plot showing all adsorption constant data for samples that have been modified with dilute TEOS.

measured diffusion coefficient, normally linear on an Arrhenius plot, to become concave to the horizontal axis (Fig. 3). Inspection of Fig. 9, however, reveals no such tendency. Figures 1 and 2 indicate that the desorption curve should show a rapid initial decrease compared to the standard ZLC model. However, the experimental curves shown in Fig.'s 8 and 11 do not convincingly show such behavior. There is therefore no evidence of the introduction of a significant surface barrier (i.e. pore mouth narrowing) as a result of the silanization procedure.

Considering model B, in which the total area available to diffusive flux is reduced by a factor α^2, it is apparent that if this model were appropriate a reduced diffusivity (relative to the parent) should be measured for the silanized catalyst samples while obtaining a constant adsorption constant in all cases. The decrease in the former is shown clearly in Fig. 9. Also, there is no apparent trend in Fig. 12; although the data are quite scattered (as discussed above) it is probably reasonable to conclude that the Henry constants of adsorption are constant across all samples.

In order to confirm the apparently good conformance to model B, it should be shown that the decrease in diffusivity tracks the decrease in surface area available for diffusive flux. The surface area data may be obtained by measuring the adsorption capacity for 4-methyl quinoline, which is too big to enter the zeolite pores, as given by temperature programmed desorption. Strictly, this gives the number of acid sites on the external surface; however, it is reasonable to assume that the fractional decrease in external acid sites indicates the fraction of the surface that has been covered with silane and thus the fraction of pore mouths that have been blocked. Thus, the measured diffusion coefficients should lie on the diagonal line shown in Fig. 13, which shows that there is at least a qualitative agreement.

The results show that, at least for the liquid phase TEOS deposition performed for the ZSM-5 samples in this work, the decrease in transport rate appears to be a result of pore mouth blocking rather than narrowing.

3.2. Sorbents Modified with Pure TEOS

Figure 14 shows the diffusional time constants measured for the sorbents modified using 100% liquid TEOS (i.e. no diluent). The data are widely scattered, although they do seem to be qualitatively consistent. Except for a single point at $T = 225$°C, the data using 4 mg of sample Z-L-100/-(60h) appear to be somewhat lower than that given when using 19 mg of the sorbent;

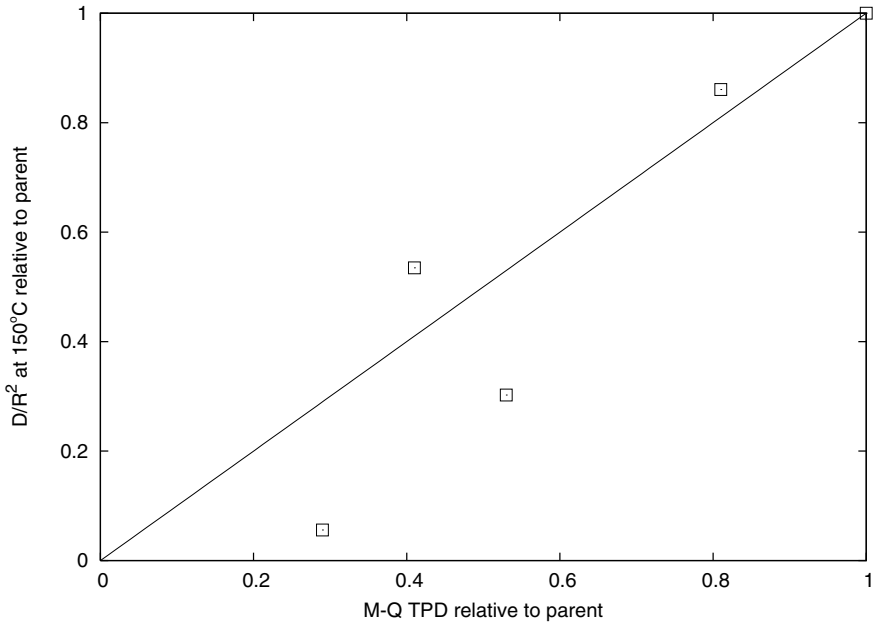

Figure 13. Diffusional time constant for cyclohexane in ZSM-5 at 150°C for modified catalyst samples (relative to parent) as a function of their 4-methyl quinoline temperature programmed desorption capacities (relative to parent). TPD data are from Weber (1998).

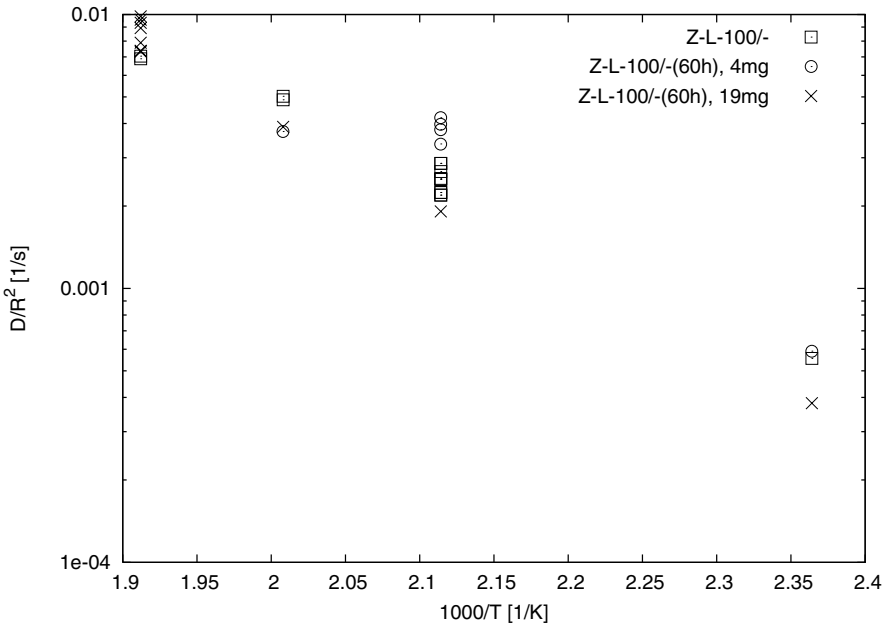

Figure 14. Arrhenius plot for ZSM-5 samples modified with pure liquid TEOS.

this effect is likely the result of a particle size distribution effect (Duncan and Möller, 2002).

Figure 15 shows four example desorption curves at identical temperatures for sample Z-L-100/-(60h), showing the effect of varying flow rate, which is qualitatively correct. Although the initial sorbate concentrations vary for these curves, Fig. 16 indicates that this parameter does not have a sig-

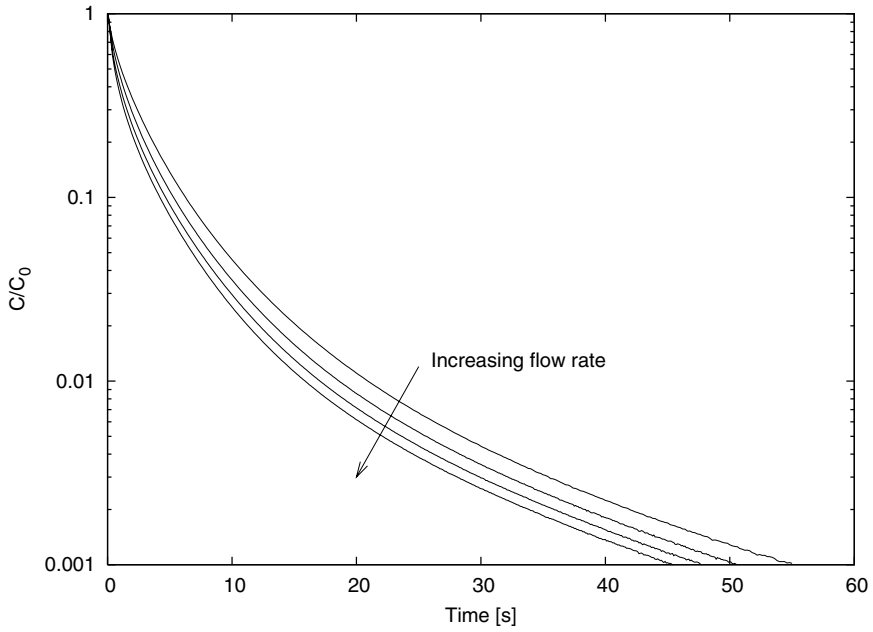

Figure 15. Desorption curves for sample Z-L-100/-(60h) at 250°C and flow rate and initial cyclohexane concentrations as follows: $F = 79.5$ ml/min, $C_0 = 207$ Pa; $F = 98.7$ ml/min, $C_0 = 167$ Pa; $F = 117.8$ ml/min, $C_0 = 140$ Pa; $F = 137.0$ ml/min, $C_0 = 120$ Pa.

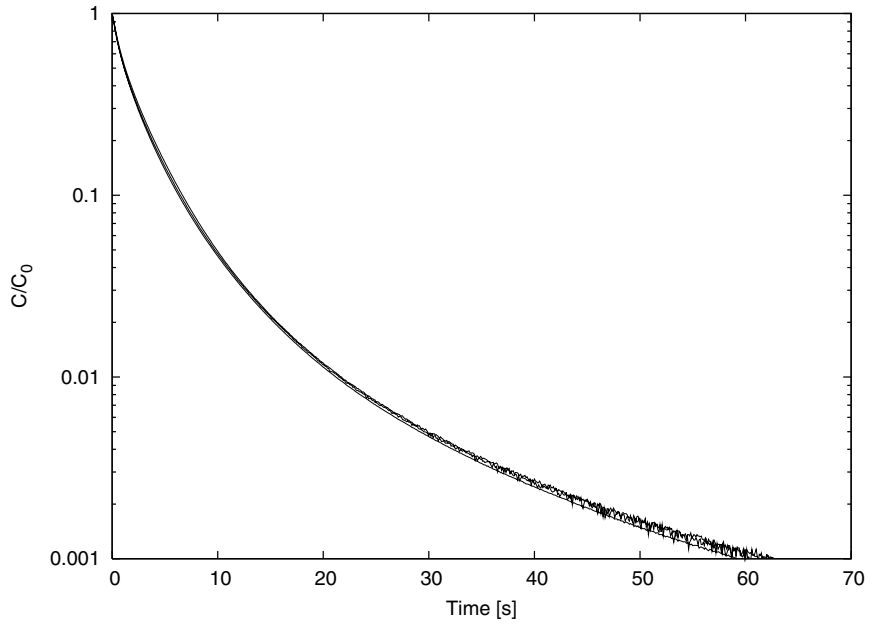

Figure 16. Desorption curves for sample Z-L-100/-(60h) at 250°C, 79.5 ml/min and initial cyclohexane concentrations of 207, 482 and 897 Pa.

nificant effect over the range considered, implying that the adsorption isotherm was probably linear for these experiments. Sample Z-L-100/- shows similar behavior.

It is evident that the desorption curves for the samples modified without the use of a diluent do not conform to the standard ZLC model, nor to the surface barrier and pore blockage variants presented above. The initial

region of the curves show a slow drop in concentration, which becomes slower with decreasing flow rate. This sort of behavior is only seen for the liquid phase model (Brandani and Ruthven, 1995), in which the accumulation of sorbate in the fluid phase cannot be neglected. Although (as pointed out above) the true initial behavior of a system with strong surface barrier resistance is likely to be an exponential decay, Eq. (14) indicates that the desorption curve should be independent of purge flow rate. As noted above, the system appears to be in the Henry region of the adsorption isotherm and the unusual shape of the desorption curves is not merely a result of changes in the equilibrium characteristics of the catalyst.

The behavior of samples Z-L-100/- and Z-L-100-(60h) cannot be reasonably explained by any model considered in this work.

4. Conclusions

The effect of depositing an inert silane compound on the external surface of ZSM-5 has been investigated both mathematically and experimentally. Two possible modifications have been considered:

1. narrowing of the pore mouths, modelled as a first order surface barrier;
2. blocking of the pore mouths, interpreted as both a reduction in area available for diffusive flux at the particle surface (model A) as well as throughout the entire particle (with no reduction in adsorption capacity) (model B).

In the surface barrier case, one would expect an analysis based on the standard ZLC model to yield a reduced value of D as well as a rapid initial drop in the desorption curve for modified sorbents. For model A, a reduction in surface area should yield an unchanged D and a reduction in K, while model B would produce a reduced D and an unchanged K.

Experiments were performed with catalyst modified by the liquid phase deposition of both pure and dilute tetraethoxy silane, the parent being Sample C of Duncan and Möller (2000). It was found that the changes in sorption behavior of the dilute modified samples corresponded most closely to the pore mouth blockage mechanism in which the area for flux is reduced throughout the particle volume (i.e. model A). This is a similar result to the statistical pore blockage model of Theodorou and Wei (1983).

The behavior of the samples modified with pure TEOS did not conform to any of the diffusion models considered.

Nomenclature

C	fluid phase sorbate concentration, mol/m^3
C_0	initial fluid phase sorbate concentration, mol/m^3
D	diffusion coefficient, m^2/s
D_{app}	apparent diffusion coefficient, m^2/s
E_{a}	diffusional activation energy, J/mol
E_{as}	surface barrier activation energy, J/mol
F	carrier fluid flow rate, m^3/s
K	Henry adsorption constant, dimensionless
K_{app}	apparent Henry adsorption constant, dimensionless
k_{s}	surface barrier mass transfer coefficient, m/s
L	constant defined by Eq. (3), dimensionless
L_{s}	analogue of L for surface barrier model, dimensionless
q	adsorbed phase sorbate concentration, mol/m^3
q_0	initial adsorbed phase sorbate concentration, mol/m^3
R	sorbent particle radius, m
R_{g}	general gas constant, J/mol/K
T	temperature, K
t	time, s
V_{s}	sorbent volume, m^3
α	fractional change in diffusion path length, dimensionless
β_n	eigenvalues defined by Eq. (4), dimensionless
β_{sn}	analogue of β_n for surface barrier model, dimensionless
τ	dimensionless time

References

Brandani, S. and D.M. Ruthven, "Analysis of ZLC Desorption Curves for Liquid Systems," *Chemical Engineering Science*, **50**(13), 2055–2059 (1995).

Čejka, J., N. Žilková, B. Wichterlová, G. Eder-Mirth, and J.A. Lercher, "Decisive Role of Transport Rate of Products for Zeolite *para*-selectivity: Effect of Coke Deposition and External Surface Silylation on Activity and Selectivity of HZSM-5 in Alkylation of Toluene," *Zeolites*, **17**, 265–271 (1996).

Duncan, W.L. and K.P. Möller, "On the Diffusion of Cyclohexane in ZSM-5 Measured by Zero-Length-Column Chromatography," *Industrial and Engineering Chemistry Research*, **39**(6), 2105–2113 (2000).

Duncan, W.L. and K.P. Möller, "The Effect of a Crystal Size Distribution on ZLC Experiments," *Chemical Engineering Science*, **57**(14), 59–70 (2002).

Eic, M. and D.M. Ruthven, "A New Experimental Technique for Measurement of Intracrystalline Diffusivity," *Zeolites*, **8**, 40–45 (1988).

Hibino, T., M. Niwa, and Y. Murakami, "Inactivation of External Surface of Mordenite and ZSM-5 by Chemical Vapour Deposition of Silicon Alkoxide," *Zeolites*, **13**, 518–523 (1993).

Hibino, T., M. Niwa, Y. Murakami, M. Sano, S. Komai, and T. Hanachai, "Structure of Deposited Germanium Dioxide which Controls the Pore-Opening Size of Mordenite," *Journal of Physical Chemistry*, **93**, 7847–7850 (1989).

Kärger, J. and D.M. Ruthven. *Diffusion in Zeolites and Other Microporous Materials*. John Wiley & Sons, Inc., New York (1992).

Kim, J.-H., A. Ishida, M. Okajima, and M. Niwa, "Modification of HZSM-5 by CVD of Various Silicon Compounds and Generation of Para-Selectivity," *Journal of Catalysis*, **161**, 387–392 (1996).

Manstein, H., K.P. Möller, W. Böhringer, and C. T. O'Connor, "Effect of the Deposition Temperature on the Chemical Vapour Deposition of Tetraethoxysilane on ZSM-5," *Microporous and Mesoporous Materials*, **51**, 35–42 (2002).

Röger, H.P., M. Krämer, K.P. Möller, and C.T. O'Connor, "Effects of In-Situ Chemical Vapour Deposition Using Tetraethoxysilane on the Catalytic and Sorption Properties of ZSM-5," *Microporous and Mesoporous Materials*, **24**(4–6), 607–614 (1998).

Röger, H.P., H. Manstein, W. Böhringer, K.P. Möller, and C.T. O'Connor, "Unravelled from the back: Kinetics of Alkoxysilane cvd on Zeolites and Evidence for Pore Mouth Plugging Determined from Model Conversion over Stepwise Silanised Samples," in *Zeolites and Mesoporous Materials at the Dawn of the 21'st Century*, A. Galarneau, F.D. Renzo, F. Fajula and J. Vedrine (Eds.), p. 142. Elsevier Science Publishers, B.V., Amsterdam (2001).

Ruthven, D.M. and S. Brandani, "Measurement of Diffusion in Microporous Solids by Macroscopic Methods," in *Physical Adsorption: Experiment, Theory and Applications*, J. Fraissard (Ed.) pp. 261–296. Kluwer Academic Publishers, The Netherlands (1997).

Theodorou, D. and J. Wei, "Diffusion and Reaction in Blocked and High Occupancy Zeolite Catalysts," *Journal of Catalysis*, **83**, 205–224 (1983).

Weber, R.W. *The Inertisation of the Zeolites ZSM-5, Mordenite and Beta by Chemical Vapour Deposition using Tetraethoxysilane*. Ph.D. thesis, University of Cape Town (1998).

Weber, R.W., K.P. Möller, and C.T. O'Connor, "The Chemical Vapour and Liquid Deposition of Tetraethoxysilane on ZSM-5, Mordenite and Beta," *Microporous and Mesoporous Materials*, **35-36**, 533–543 (2000).